

Chiral symmetry and strangeness at SIS energies

Matthias F.M. Lutz,
Gesellschaft für Schwerionenforschung GSI, Postfach 110552
D-64220 Darmstadt, Germany

November 10, 2018

Abstract

In this talk we review the consequences of the chiral SU(3) symmetry for strangeness propagation in nuclear matter. Objects of crucial importance are the meson-baryon scattering amplitudes obtained within the chiral coupled-channel effective field theory. Results for antikaon and hyperon-resonance spectral functions in cold nuclear matter are presented and discussed. The importance of the $\Sigma(1385)$ resonance for the subthreshold antikaon production in heavy-ion reaction at SIS is pointed out. The in-medium properties of the latter together with an antikaon spectral function based on chiral SU(3) dynamics suggest a significant enhancement of the $\pi \Lambda \rightarrow \bar{K} N$ reaction in nuclear matter.

1 Introduction

The foundation of all theoretical attempts to describe and possibly predict hadron properties in a dense nuclear environment should be Quantum Chromo Dynamics (QCD), the fundamental theory of strong interactions. The QCD Lagrangian predicts all hadron interactions in terms of quark and gluon degrees of freedom. At large momentum transfers QCD is extremely successful and predictive, because observable quantities can be evaluated perturbatively in a straightforward manner. At small momentum transfers, in contrast, QCD is less predictive so far due to its non-perturbative character. It is still an outstanding problem to systematically unravel the properties of QCD in its low-energy phase where the effective degrees of freedom are hadrons rather than quarks and gluons. That is a challenge since many of the most exciting phenomena of QCD, like the zoo of meson and baryon resonances, manifest themselves at low-energies. Also the fundamental question addressed in this talk 'how do hadrons change their properties in dense nuclear matter' requires a solid understanding of QCD at small momentum transfer.

There are two promising paths along which one achieved and expects further significant progress. A direct evaluation of many observable quantities is possible by large scale numerical simulations where QCD is put on a finite lattice [1]. Though many static properties, like hadron ground-state properties, have been successfully reproduced by lattice calculations, the description of the wealth of hadronic scattering data is still outside the scope of that approach [1]. Also the determination of hadron properties at finite and cold nuclear densities is still not feasible on the lattice [2, 3]. Here a complementary approach, effective field theory, is more promising at present. Rather than solving low-energy QCD in terms of quark and gluon degrees of freedom, inefficient at low energies, one aims at constructing an effective quantum field theory in terms of hadrons directly. The idea is to constrain that theory by as

many properties of QCD as possible and establish a systematic approximation strategy. This leads to a significant parameter reduction and a predictive power of the effective field theory approach.

An effective field theory, which meets the above criteria, is the so called Chiral Perturbation Theory (χ PT) applicable in the flavor $SU(2)$ sector of low-energy QCD [4]. This effective field theory is based on a simple observation, namely that QCD is chirally symmetric in the limiting case where the up and down current quark masses vanish $m_{u,d} = 0$. This implies in particular that the handedness of quarks is a conserved property in that limit. There is mounting empirical evidence that the QCD ground state breaks the chiral $SU(2)$ symmetry spontaneously in the limit $m_{u,d} = 0$. For instance the observation that hadrons do not occur in parity doublet states directly reflects that phenomenon. Also the smallness of the pion masses with $m_\pi \simeq 140$ MeV much smaller than the nucleon mass $m_N \simeq 940$ MeV, naturally fits into this picture once the pions are identified to be the Goldstone bosons of that spontaneously broken chiral symmetry. The merit of standard χ PT is first, that it is based on an effective Lagrangian density constructed in accordance with all chiral constraints of QCD and second, that it permits a systematic evaluation applying formal power counting rules [4]. In χ PT the finite but small values of the up and down quark masses $m_{u,d} \simeq 10$ MeV are taken into account as a small perturbation defining the finite masses of the Goldstone bosons. The smallness of the current quark masses on the typical chiral scale of 1 GeV explains the success of standard χ PT.

It is of course tempting to generalize the chiral $SU(2)$ scheme to the $SU(3)$ flavor group which includes the strangeness sector, the main theme of this talk. To construct the appropriate chiral $SU(3)$ Lagrangian is mathematically straightforward and has been done long ago (see e.g. [4]). The mass $m_s \simeq (10 - 20) m_{u,d}$ of the strange quark, though much larger than the up and down quark masses, is still small on the typical chiral scale of 1 GeV. The required approximate Goldstone boson octet is readily found with the pions, kaons and the eta-meson. Nevertheless, important predictions of standard χ PT as applied to the $SU(3)$ flavor group are in stunning conflict with empirical observations. Most spectacular is the failure of the Weinberg-Tomozawa theorem [5, 6] which predicts an attractive K^- -proton scattering length, rather than the observed large and repulsive value. Progress can be made upon accepting a crucial observation that the power counting rules must not be applied to a certain subset of Feynman diagrams. Whereas for irreducible diagrams the chiral power counting rules are well justified, this is no longer necessarily the case for the irreducible diagrams [7]. The latter diagrams are enhanced as compared to irreducible diagrams and therefore require a systematic resummation scheme in particular in the strangeness sectors. The χ -BS(3) approach, which is based on the coupled-channel Bethe-Salpeter scattering equation, was developed in great detail over the last years [8, 9, 10]. It constitutes a rigorous effective field theory based on the above ideas. All results presented and discussed in this talk are based on computations within the χ -BS(3) approach.

Once the microscopic interaction of the Goldstone bosons with the constituents of nuclear matter is understood one may study the properties of Goldstone bosons in nuclear matter. Not only from an experimental but also from a theoretical point of view the pions and kaons, the lightest excitation of the QCD vacuum with masses of 140 MeV and 495 MeV respectively, are outstanding probes for exciting many-body dynamics. The Goldstone bosons are of particular interest since their in-medium properties reflect the structure of the nuclear many-body ground state. For example at high baryon densities one expects the chiral symmetry to be restored. One therefore anticipates that the Goldstone bosons change their properties substantially as one compresses nuclear matter.

Even though in the $SU(3)$ limit of QCD with degenerate current quark masses $m_u = m_d = m_s$ the pions and kaons have identical properties with respect to the strong interactions, they provide very different means to explore the nuclear many-body system. This is because the $SU(3)$ symmetry is explicitly broken by a nuclear matter state with strangeness density zero, a typical property of matter produced in the laboratory. A pion, if inserted into isospin degenerate nuclear matter, probes rather directly the spontaneously broken or possibly restored chiral $SU(2)$ symmetry. A kaon, propagating in strangeness free nuclear matter, loses its Goldstone boson character since the matter by itself explicitly

breaks the $SU(3)$ symmetry. It is subject to three different phenomena: the spontaneously broken chiral $SU(3)$ symmetry, the explicit symmetry breaking of the small current quark masses and the explicit symmetry breaking of the nuclear matter bulk. The various effects are illustrated by recalling the effective pion and kaon masses in a dilute isospin symmetric nuclear matter gas. The low-density theorem [11, 12] predicts mass changes Δm_Φ^2 for any meson Φ in terms of its isospin averaged s-wave meson-nucleon scattering length $a_{\Phi N}$

$$\Delta m_\Phi^2 = -4\pi \left(1 + \frac{m_\Phi}{m_N}\right) a_{\Phi N} \rho + \mathcal{O}(\rho^{4/3}) \quad (1)$$

where ρ denotes the nuclear density. According to the above arguments one expects that the pion-nucleon scattering length $a_{\pi N} \propto m_\pi^2$ must vanish in the chiral $SU(2)$ limit since isospin symmetric nuclear matter conserves the Goldstone boson character of the pions at least at small densities. On the other hand, kaons loose their Goldstone boson properties and therefore one expects $a_{KN} \propto m_K$ and in particular $a_{K^-N} \neq a_{K^+N}$. This is demonstrated by the Weinberg-Tomozawa theorem which predicts the s-wave scattering length in terms of the chiral order parameter $f_\pi \simeq 93$ MeV :

$$a_{\pi N} = 0 + \mathcal{O}(m_\pi^2) , \quad a_{K^\pm N} = \mp \frac{m_K}{4\pi f_\pi^2} + \mathcal{O}(m_K^2) . \quad (2)$$

In the pion sector the Weinberg-Tomozawa theorem (2) is beautifully confirmed by the smallness of the empirical isospin averaged pion-nucleon scattering length $a_{\pi N} \simeq -0.01$ fm. In the kaon sector the Weinberg-Tomozawa theorem misses the empirical scattering K^+ nucleon scattering length $a_{K^+N} \simeq -0.3$ fm by about a factor of three. Even more spectacular is the disagreement of Weinberg-Tomozawa term in the K^- case where (2) predicts $a_{K^-N} \simeq +0.9$ fm while the empirical K^- nucleon scattering length is about $a_{K^-N} \simeq (-0.6 + i1.1)$ fm. Whereas in conjunction with the low-density theorem the Weinberg-Tomozawa theorem predicts a decreased effective K^- mass, the empirical scattering length unambiguously states that there must be repulsion in the K^- channel at least at very small nuclear densities. The antikaon-nucleon scattering process is complicated due to the open inelastic $\pi\Sigma$ and $\pi\Lambda$ channels. This is reflected in the large imaginary part of the empirical K^- nucleon scattering length. A quite rich variety of phenomena arises from the presence of both the s-wave $\Lambda(1405)$ and p-wave $\Sigma(1385)$ resonances just below, and the d-wave $\Lambda(1520)$ resonance not too far above the antikaon-nucleon threshold.

In nuclear matter there exist multiple modes with quantum numbers of the K^- resulting from the coupling of the various hyperon states to a nucleon-hole state [13]. As a consequence the K^- spectral function shows a rather complex structure as a function of baryon density, kaon energy and momentum. This is illustrated by recalling the low-density theorem as applied for the energy dependence of the kaon self energy $\Pi_{\bar{K}}(\omega, \rho)$. At zero antikaon momentum the latter,

$$\Pi_{\bar{K}}(\omega, \rho) = -4\pi \left(1 + \frac{\omega}{m_N}\right) f_{\bar{K}N}^{\text{s-wave}}(m_N + \omega) \rho + \mathcal{O}(\rho^{4/3}) , \quad (3)$$

is determined by the s-wave kaon-nucleon scattering amplitude $f_{\bar{K}N}^{\text{s-wave}}(\sqrt{s})$. A pole contribution to $\Pi_{\bar{K}}(\omega, \rho)$ from a hyperon state with mass m_H , if sufficiently strong, may lead to a K^- like state of approximate energy $m_H - m_N$. Most important are the $\Lambda(1405)$ s-wave resonance and the $\Sigma(1385)$ p-wave resonance. An attractive modification of the antikaon spectral function was already anticipated in the 70's by the many K-matrix analyses of antikaon-nucleon scattering (see e.g. [14]) which predicted considerable attraction in the subthreshold s-wave K^- nucleon scattering amplitudes. In conjunction with the low-density theorem (3) this leads to an attractive antikaon spectral function in nuclear matter. As was pointed out first in [15] the realistic evaluation of the antikaon self energy in nuclear matter requires a self-consistent scheme. In particular the feedback effect of an attractive antikaon spectral function on the antikaon-nucleon scattering process was found to be important for the $\Lambda(1405)$ resonance structure in nuclear matter.

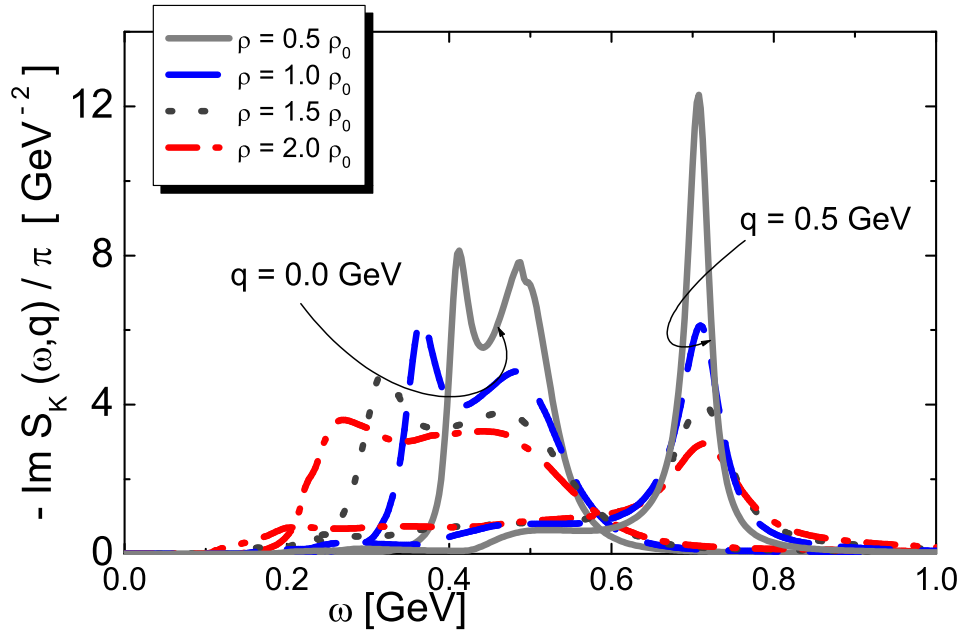


Figure 1: Antikaon spectral function at momentum $q = 0$ MeV and $q = 500$ MeV and various nuclear matter densities. The results are based on the computation presented in [26].

2 Antikaons and hyperon resonances at SIS energies

The quantitative evaluation of the antikaon spectral function in nuclear matter is a challenging problem. It should be based on a solid understanding of the antikaon-nucleon scattering process in free space. Based on a description of the data set one obtains a set of antikaon-nucleon scattering amplitudes. The present data set for antikaon-nucleon scattering leaves much room for different theoretical extrapolations to subthreshold energies [14, 16, 17, 18, 19, 20, 21, 22, 23, 24, 25]. As a consequence the subthreshold $\bar{K}N$ scattering amplitudes of different analyses may differ by as much as a factor of two [23, 24] in the region of the $\Lambda(1405)$ resonance. Thus it is of crucial importance to apply effective field theory methods in order to control the uncertainties. In particular constraints from crossing symmetry and chiral symmetry should be taken into account. In Fig. 1 the antikaon spectral function at momenta $q = 0$ MeV and $q = 500$ MeV evaluated at several nuclear densities is shown [26]. The results are based on antikaon-nucleon scattering amplitudes obtained within the chiral coupled-channel effective field theory [9], where s-, p- and d-wave contributions were considered. The many-body computation [26] was performed in a self-consistent manner respecting in addition constraints arising from covariance. Fig. 1 illustrates that at zero momentum the spectral function acquires a rather broad distribution as the nuclear density increases, with support significantly below the free-space kaon mass. This reflects the opening of many inelastic channels. In nuclear matter the antikaon couples strongly to hyperon-resonance nucleon-hole states. Most important are the $\Lambda(1405)$ and $\Sigma(1385)$ resonances. At moderate momenta $q = 500$ MeV the spectral function looks significantly different as compared to the one at $q = 0$ MeV. It is characterized by a peak close to $\omega = \sqrt{m_K^2 + q^2}$ and a pronounced low-energy tail. As the density increases the strength in the peak diminishes shifting more and more strength into the low-energy tail.

Of interest are the implications of results for antikaon and hyperon-resonance spectral distributions in cold nuclear matter for subthreshold antikaon production in heavy-ion reaction at SIS energies. Strictly

speaking such results do not apply for the conditions present inside a fireball created after the collision of two heavy nuclei. The quantitative description of such a process requires a transport theoretical description capable to model physics of finite systems off equilibrium. The latter requires as input hadronic cross sections, or more precisely hadronic transition rates, that are taken from experiment or theory. Calculations performed in the idealized world of infinite but hot and dense nuclear matter are nevertheless a useful tool to discuss and understand effects on a qualitative level. In certain channels transition rates that are typically derived from free-space cross sections may be significantly changed in a hot and dense nuclear environment.

One may argue that if the antikaon spectral function evaluated for infinite hot nuclear matter shows considerable strength at energies smaller than the free kaon mass, it is energetically easier to produce antikaons in a fireball than if the effective antikaon mass distribution was not reduced. In this case one may expect to see some type of enhancement of antikaon production rates. It is a challenge to verify the above simple but physical interpretation of the observed kaon and antikaon yields in terms of transport model simulations. In [27] results of the KaoS collaboration for the kaon and antikaon transverse spectra for Au+Au at $E_{\text{beam}}=1.5$ AGeV are shown. The spectra shown are typical for most observed particle multiplicities. They are fitted well by a simple Boltzmann distribution

$$\sim \exp \left(- (E_{cm} - m_K)/T \right), \quad (4)$$

in terms of an effective temperature parameter T . The effective temperatures of the K^+ are about 20 MeV larger than the ones for the K^- [27]. It is important to realize that the Boltzmann type behavior of the spectra does not imply that the kaons and antikaons are necessarily equilibrated. Estimates for the kaon mean free path, which are based on the empirical kaon-nucleon cross section, suggest that the kaons do not have a chance to reach equilibrium conditions in a typical heavy-ion collision at SIS energies. That may be different for antikaons as will be discussed in some detail below.

Since at subthreshold energies the mean energy available by one nucleon is not sufficient to produce an antikaon in an elementary nucleon-nucleon collision by definition, one visualizes the production process to occur in a series of successive reactions [28, 29, 30, 31],

$$N N \rightarrow N \Delta \rightarrow N N \pi, \quad N N \rightarrow N Y K, \quad \pi Y \rightarrow \bar{K} N, \quad (5)$$

where $Y = \Lambda(1115), \Sigma(1185)$. Here we do not intend to provide a complete listing of reactions included in transport model simulations rather we would like to discuss the main effects qualitatively. A heavy-ion reaction produces, besides photons and leptons, dominantly pions, the lightest hadronic degrees of freedom available. For SIS energies at GSI this production is thought to be driven by the isobar production process $N N \rightarrow N \Delta \rightarrow N N \pi$. The kaon production is determined by the primary $N N \rightarrow N Y K$ reaction far above threshold but by the secondary reaction $\pi N \rightarrow K Y$ at subthreshold energies. Because of strangeness conservation the antikaon production threshold in nucleon-nucleon collisions is much larger than the threshold of kaon production. The former is determined by the $N N \rightarrow N N K \bar{K}$ reaction leading to

$$\sqrt{s_{\text{thres}}^{(\bar{K})}} - \sqrt{s_{\text{thres}}^{(K)}} = m_K + m_N - m_\Lambda \simeq 320 \text{ MeV}. \quad (6)$$

It is therefore plausible that antikaons are dominantly produced in the secondary $\pi Y \rightarrow \bar{K} N$ reaction in particular at subthreshold energies. Consequently these reactions received considerable attention in the study of subthreshold antikaon production [28, 29, 32]. A clear hint that the antikaon production in nucleus-nucleus collisions is indeed driven by the secondary $\pi Y \rightarrow \bar{K} N$ reaction follows from the centrality dependence of the measured ratio K^-/K^+ [27]. The number of nucleons, A_{part} that participate in a Ni on Ni or Au on Au collision is a measure for the inverse size of the impact parameter. Since both, the kaon and antikaon yields depend strongly on the impact parameter [33] the empirical observation

that the ratio of the yields is almost insensitive to it signals that the production mechanisms of the kaons and antikaons must be strongly related.

So far most transport model simulations of antikaon production rely on rough approximations. For instance the complicated antikaon spectral function is substituted by a quasi-particle ansatz parameterized in terms of an effective antikaon mass that drops basically linearly with the nuclear density [28, 29]. Technically this is implemented by incorporating an appropriate mean field modifying the trajectories of the antikaon between collisions in the fireball. The width of the quasi particle is then modelled by including the inelastic cross sections like $\bar{K}N \rightarrow \pi Y$. For cross sections involving antikaons in initial or final states simple substitution rules like e.g. $\sqrt{s} \rightarrow \sqrt{s} - \Delta m_{\bar{K}}$ are applied. Such computations confirm the expectation that the antikaon yield is quite sensitive to an attractive mean field of the antikaon [28, 29]. Runs where an attractive mean field and the absorption cross sections are both switched off or on are reported to be fairly close to the measured multiplicities [28, 29]. Neglecting, however the attractive mean field but including the antikaon absorption cross sections underestimates the antikaon yield up to a factor 5 [28, 29].

A more sophisticated simulation was performed by Schaffner, Effenberger and Koch [32] in which the consequences of two effects were studied. First, the effect of in-medium modifications of the $\pi Y \rightarrow \bar{K}N$ reactions was studied. And second, a momentum dependence of the antikaon potential was considered. The momentum dependence was chosen such that at moderate antikaon momenta of about 300-400 MeV the attractive mean field was basically switched off. This was motivated by microscopic many-body evaluations of the antikaon self energy which predicted that type of behavior [15]. The in-medium modification of the production cross sections $\pi Y \rightarrow \bar{K}N$ were assumed to be dominated by the Pauli blocking effect [34] that shifts the $\Lambda(1405)$ resonance from $\sqrt{s} = 1405$ MeV to larger energies, about $\sqrt{s} \simeq 1490$ MeV at nuclear saturation density. As a consequence the authors report an enhancement factor for the $\pi\Sigma \rightarrow \bar{K}N$ reaction of about 20 close to $\sqrt{s} = 1490$ MeV. Both effects, the attractive mean field and the increased $\pi Y \rightarrow \bar{K}N$ cross section gave rise to a similar effects in the antikaon yield. Together the two mechanism predict an enhancement factor of about 4 as compared to a computation that applies the empirical cross sections and discards any mean-field effects. However, as was pointed out by Schaffner, Effenberger and Koch [32], once the momentum dependence of the attractive mean field was incorporated together with the fact that in their model the enhancement of the cross section disappears already at moderate temperatures $T \simeq 80$ MeV, the results are quite close to the reference calculation with no medium effects. All together the empirical antikaon yields are not described, they are underestimated by about a factor 3-4.

In a more recent work by Aichelin, Hartnack and Oeschler [30, 31] a further interesting aspect was emphasized. Since the antikaon production is driven by the $\pi Y \rightarrow \bar{K}N$ reaction the total antikaon yield should be sensitive to the kaon production mechanism. This follows since the number of kaons and hyperons available are comparable due to the typical production reaction (5). A repulsive mass shift for the kaon can therefore compensate for the effect implied by an attractive mean field for the antikaon. We would argue, however, that the computation by Aichelin and Hartnack [30] most likely overemphasizes this effect due to a too large mass shift for the kaon (about 70 MeV at $2\rho_0$). This objection is based on a recent calculation based on the kaon-nucleon s- and p-wave phase shifts [35] demonstrating that a kaon produced with momenta of about 400 MeV at $2\rho_0$ the repulsive mass shift is only about 45 MeV, much smaller than the value of 70 MeV used in [30]. The conclusions of Aichelin, Hartnack and Oeschler [30, 31] depend also sensitively on the magnitude of the attractive mean fields for the nucleons and hyperons as well as on the poorly known $N\Delta \rightarrow NYK$ reaction rates. In order to reduce such uncertainties it would be useful to describe not only total yields of kaons, antikaons and hyperons but at the same time achieve quantitative agreement with the azimuthal emission pattern [36, 37, 38]. Aichelin, Hartnack and Oeschler [30, 31] affirm that the K^-/K^+ ratio is rather insensitive to the details of the kaon production and therefore should be considered as a superior observable to test the antikaon dynamics. However, their claim, that including an attractive mean field for the antikaon into

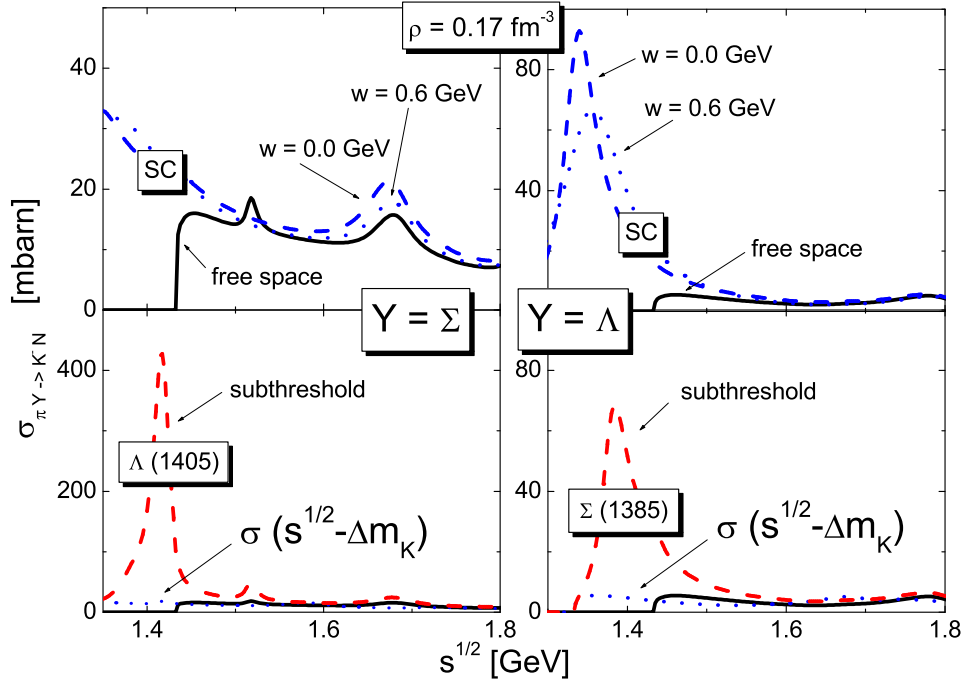


Figure 2: The upper panels show the pion induced cross sections of antikaons obtained in a self-consistent many-body evaluation (dashed for $\vec{w} = 0$ MeV and dotted lines for $\vec{w} = 600$ MeV) at nuclear saturation density as compared to the free-space cross sections (full lines). The lower panels give the results of schematic evaluations. The dotted lines are the free-space cross section shifted in \sqrt{s} by $\Delta m_{\bar{K}} = -100$ MeV. The dashed lines follow with computations that are based on the subthreshold free-space amplitudes as predicted by the χ -BS(3) approach together with a final state phase space evaluated with a reduced kaon mass.

the simulation does not affect the total antikaon yield, remains puzzling. This contradicts the typical enhancement factors 2-4 as were obtained in previous simulations [28, 29, 39, 32]. In their work [31] the possible importance of in-medium modified cross sections is studied. Within their scenario, which does not consider a momentum dependence of the antikaon mean field, they observe an enhancement of the K^-/K^+ ratio by a factor 2 if the $\pi Y \rightarrow \bar{K}N$ cross sections are enlarged uniformly by a factor three. However, the impact parameter dependence of that ratio is affected strongly by this ad-hoc procedure leading to a dependence that appears incompatible with the behavior shown in [27]. It is argued that the antikaons are produced at a late stage of the collision even though the difference of absorption and production rates shows a clear maximum in the high density ($\rho > 1\rho_0$) initial phase. Increasing the $\pi Y \rightarrow \bar{K}N$ cross sections only affects the antikaon absorption process at the late stage of the fireball expansion since the typical pions and hyperons do not have sufficient kinetic energy to produce antikaons anymore. This would lead to a drop of the K^-/K^+ ratio with increasing impact parameter.

The above discussion implies that it is important to obtain an improved understanding of the $\pi Y \rightarrow \bar{K}N$ cross sections as they may change in a nuclear environment [32]. To the extent that the latter reaction is of crucial importance for the subthreshold antikaon production at SIS energies, chiral symmetry plays a decisive role in the understanding of the antikaon yield in heavy-ion reactions. In Fig. 2 the result of a computation based on the self-consistent scheme introduced in [26, 40] are presented.

In the upper panel we show the isospin averaged $\pi\Sigma \rightarrow \bar{K}N$ and $\pi\Lambda \rightarrow \bar{K}N$ cross sections where the in-medium scattering amplitudes are used together with the antikaon spectral function defining the final-state phase space. The latter ones are taken from [9, 26]. Comparing the solid with the dashed and dotted lines one realizes a dramatic enhancement for the $\pi\Lambda$ reaction but a much more moderate enhancement for the $\pi\Sigma$ reaction. The dashed and dotted lines correspond to the situation where the sum of initial three-momenta is 0 MeV and 600 MeV respectively. To explain the source of this effect the figure shows in its lower panel the same cross sections evaluated in two different schematic ways. The dotted lines give the result obtained according to the prescription $\sqrt{s} \rightarrow \sqrt{s} - \Delta m_{\bar{K}}$ as commonly applied in transport model simulations. It is used $\Delta m_{\bar{K}} = -100$ MeV typically for the amount of attraction found for the antikaon at saturation density. The cross sections remain as small as they are in free-space. A striking enhancement is shown by the dashed lines in the lower panel. Here we use the free-space scattering amplitude and evaluate the cross section with the final state phase space determined by a reduced kaon mass of 394 MeV. As a result this cross section probes the scattering amplitudes at subthreshold energies a kinematical region where they are not directly constrained by the scattering data. Since the χ -BS(3) scheme predicts considerable strength in the subthreshold amplitudes from the s-wave $\Lambda(1405)$ and p-wave $\Sigma(1385)$ resonances the former cross sections are dramatically enhanced as compared to the free-space cross sections. Comparing the lower with the upper panel demonstrates that the latter cross section, though providing a simple physical interpretation of the enhancement, do not adequately reproduce the full computation as it arises in a self-consistent framework. In particular the large cross section of the $\pi\Sigma \rightarrow \bar{K}N$ reaction predicted by the free-space amplitudes is significantly reduced in the self-consistent scheme. Here one should note that the s-wave and p-wave final-state phase space factors probe the antikaon spectral function in different ways. Thus, the net result is a combined effect depending on the in-medium amplitude and a projection of the antikaon spectral function that depends on the angular momentum.

The moderate enhancement for the $\pi\Sigma \rightarrow \bar{K}N$ reaction confirms the results of our previous work [15], in which it was pointed out that a self-consistent antikaon dynamics does not generate the large enhancement factor predicted by a scheme that considers Pauli blocking only [34, 32]. Since an enhancement factor that is driven by the Pauli blocking effect will eventually disappear once a finite temperature is allowed for, it can not explain enlarged cross sections to be used in heavy-ion reactions in any case. The striking effect induced by the $\Sigma(1385)$ resonance in the $\pi\Lambda \rightarrow \bar{K}N$ reaction is novel. It is the result of our detailed analysis of the kaon and antikaon scattering data which predicts that there is a strong coupling of the $\Sigma(1385)$ resonance to the $\pi\Lambda$ and $\bar{K}N$ channels at subthreshold energies. The self-consistent many-body computation presented here suggests that this strong coupling persists in the nuclear medium giving rise to the large enhancement factor found for the in-medium $\pi\Lambda \rightarrow \bar{K}N$ reaction. This effect should have important consequences for the antikaon yield in nucleus-nucleus collisions at SIS energies.

As demonstrated in [31] the ad-hoc increase of the $\pi Y \rightarrow \bar{K}N$ cross section away from its free-space limit does increase the total antikaon yield. This demonstrates that transport model simulations of the antikaon yield that are based on free-space cross sections do not reach equilibrium conditions. Of course beyond some critical enhancement factor one would expect the yield to saturate implying that phase space is populated statistically. To put it in another way an enhancement factor 40 will not increase the yield by a factor of 40. However, we argue that a strong enhancement factor is rather welcome since that implies that the enhancement should be strong enough exceeding the critical value required for driving the antikaons towards equilibrium conditions even at smaller density or equivalently larger impact parameter. Therefore we would expect that the impact parameter dependence of the K^-/K^+ yield should be weak as seen [27] and predicted by the statistical model of Cleymans, Oeschler and Redlich [41]. Here we would deviate from the line of arguments put forward by Aichelin, Hartnack and Oeschler who argued that with their ad-hoc enhancement the impact parameter dependence of the K^-/K^+ yield decreases with increasing impact parameter. Since the unscaled cross sections predict a

flat behavior in their simulation, more consistent with [27], one may favor the free-space cross sections. This conclusion would be based, however, on a simple energy independent enhancement factor of the $\pi Y \rightarrow \bar{K} N$ transition rate. In contrast Fig. 2 suggests that even at a rather late stage of the fireball expansion the pions and hyperons need very little kinetic energy to produce a virtual antikaon. That should lead to a flattening of the number of antikaons with increasing reaction time contradicting the results shown by Aichelin, Hartnack and Oeschler [31].

It would be very useful to incorporate the dynamics of the $\Sigma(1385)$ into transport model simulations. For a first attempt see [42]. If it can be confirmed that the description of the antikaon yield requires an in-medium enhancement of the $\pi Y \rightarrow \bar{K} N$ rates we would interpret this as a clear signal for an attractive shift in the antikaon mass distribution. Only if the in-medium $\bar{K} N$ phase space has significant overlap with the $\Sigma(1385)$ resonance the $\pi \Lambda \rightarrow \bar{K} N$ rate can be enhanced significantly.

3 Conclusion

We reviewed the relevance of the chiral SU(3) symmetry for subthreshold antikaon production in heavy-ion collisions [43]. It is argued that chiral symmetry plays a decisive role since it helps to control the complicated interaction of antikaons with the constituents of matter. Results, that are based on the chiral coupled-channel effective field theory, have interesting consequences for antikaon propagation in dense nuclear matter. For the antikaon spectral function a pronounced dependence on the three-momentum of the antikaon is predicted. The spectral function shows typically a rather wide structure invalidating a simple quasi-particle description. For instance at $\rho = 0.17 \text{ fm}^{-3}$ the strength starts at the quite small energy, $\omega \simeq 200 \text{ MeV}$. Furthermore, at nuclear saturation density attractive mass shifts for the $\Lambda(1405)$, $\Sigma(1385)$ and $\Lambda(1520)$ are foreseen. The hyperon states are found to show at the same time moderately increased decay widths.

The importance of the p-wave $\Sigma(1385)$ resonance for the antikaon production in heavy ion collisions as studied at GSI was pointed out. The presence of the latter resonance implies a substantially enhanced $\pi \Lambda \rightarrow \bar{K} N$ reaction rate in nuclear matter. Contrary to naive expectations only a small enhancement of the $\pi \Sigma \rightarrow \bar{K} N$ reaction was derived even though it couples to the s-wave $\Lambda(1405)$ resonance. It was emphasized that the incorporation of the $\Sigma(1385)$ resonance into transport model simulations of nucleus-nucleus collisions at SIS energies should help to obtain a quantitative and microscopic understanding of the empirical antikaon yields. To help understanding this dynamics it is desirable to measure the $\Sigma(1385)$ yield at SIS energies.

References

- [1] F. Karsch, *Nucl. Phys. B (Proc. Suppl.)* 83-84 (2000) 14 .
- [2] G. Boyd, et al. *Phys. Lett. B* 349 (1995) 170 .
- [3] T. Hatsuda, hep-ph/0104139.
- [4] S. Weinberg, *The quantum theory of fields*, Vol. II, University Press, Cambridge (1996).
- [5] S. Weinberg, *Phys. Rev. Lett.* 17 (1966) 616 .
- [6] Y. Tomazawa, *Nuov. Cim. A* 46 (1966) 707 .
- [7] S. Weinberg, *Phys. Lett. B* 251 (1990) 288 .
- [8] M. Lutz and E. Kolomeitsev, in *Proc. of 28th Int. Workshop on Gross Properties of Nuclei and Nuclear Excitations: Hadrons in Dense Matter*, Hirschegg, Austria, 16-22 January 2000.
- [9] M.F.M. Lutz and E.E. Kolomeitsev, *Nucl. Phys. A* 700 (2002) 193 .
- [10] M.F.M. Lutz und E.E. Kolomeitsev, nucl-th/0307039.

- [11] C.D. Dover, J. Hüfner and R.H. Lemmer, *Ann. Phys.* 66 (1971) 248 .
- [12] M. Lutz, A. Steiner and W. Weise, *Nucl. Phys. A* 574 (1994) 755 .
- [13] E.E. Kolomeitsev, D.N. Voskresensky and B. Kämpfer, *Nucl. Phys. A* 588 (889) 1995 .
- [14] A.D. Martin, *Nucl. Phys. B* 179 (1981) 33 .
- [15] M. Lutz, *Phys. Lett. B* 426 (1998) 12 ; M.F.M. Lutz, in Proceedings "APCTP Workshop on Astro-Hadron Physics", Seoul, 25.- 31. Oktober 1997, World Scientific 1999.
- [16] B.R. Martin and M. Sakit, *Phys. Rev.* 183 (1969) 1352 .
- [17] J.K. Kim, *Phys. Rev. Lett.* 14 (1965) 29 .
- [18] M. Sakit et al., *Phys. Rev.* 139 (1965) B719 .
- [19] G.P. Gopal et al. *Nucl. Phys.* 119 (1977) 362 .
- [20] G. C. Oades, in Proc. of *Int. Workshop on Low and Intermediate-Energy Kaon-Nucleon Physics*, Rome, Italy, 24-28 March 1980, (eds. E. Ferrari, G. Violini), D. Reidel Publishing, Dordrecht (1980).
- [21] A. Müller-Groeling, K. Holinde and J. Speth, *Nucl. Phys. A* 513 (1990) 557 .
- [22] R.H. Dalitz and A. Deloff, *J. Phys. G* 17 (1991) 289 .
- [23] N. Kaiser, P.B. Siegel and W. Weise, *Nucl. Phys. A* 594 (1995) 325 ;
N. Kaiser, T. Waas and W. Weise, *Nucl. Phys. A* 612 (1997) 297 .
- [24] E. Oset and A. Ramos, *Nucl. Phys. A* 635 (1998) 99 .
- [25] M.Th. Keil, G. Penner and U. Mosel, *Phys. Rev. C* 63 (2001) 045202 .
- [26] M.F.M. Lutz and C.L. Korpa, *Nucl. Phys. A* 700 (2002) 309 .
- [27] A. Förster for the KaoS Collaboration, nucl-ex/0202010, nucl-ex/0307017.
- [28] W. Cassing et al., *Nucl. Phys. A* 614 (1997) 415 .
- [29] G.Q. Li and G.E. Brown, *Phys. Rev. C* 58 (1998) 1698 .
- [30] J. Aichelin and Ch. Hartnack, *J. Phys. G* 27 (2001) 571 .
- [31] J. Aichelin, H. Oeschler and Ch. Hartnack, *Phys. Rev. Lett.* 90 (2003) 102302 .
- [32] J. Schaffner-Bielich, V. Koch and M. Effenberger, *Nucl. Phys. A* 669 (2000) 153 .
- [33] M. Menzel et al., *Phys. Lett. B* 495 (2000) 26 .
- [34] V. Koch, *Phys. Lett. B* 337 (1994) 7 .
- [35] M.F.M. Lutz, E.E. Kolomeitsev and C.L. Korpa, *J. Phys. G* 28 (2002) 1729 .
- [36] G.Q. Li, C.M. Ko and B.A. Li, *Phys. Rev. Lett.* 74 (1995) 235 .
- [37] Z.S. Wang et al., *Eur. Phys. J. A* 5 (1999) 275 .
- [38] E. L. Bratkovskaya, W. Cassing and U. Mosel, *Nucl. Phys. A* 622 (1997) 593 .
- [39] W. Cassing and E.L. Bratkovskaya, *Phys. Rep.* 308 (1999) 65 .
- [40] M.F.M. Lutz, GSI-Habil-2002-1.
- [41] J. Cleymans, H. Oeschler and K. Redlich, *Phys. Lett. B* 485 (2000) 27 .
- [42] W. Cassing, L. Tolos, E. L. Bratkovskaya and A. Ramos, *Nucl. Phys. A* 727 (2003) 59 .
- [43] F. Laue, Ch. Sturm et al., *Phys. Rev. Lett.* 82 (1999) 1640 .